Degeneration of basal and limbic networks is a core feature of behavioural variant frontotemporal dementia

Vesna Vuksanović,[1,2,4] Roger T. Staff,[3] Suzannah Morson,[4,5] Trevor Ahearn,[3] Luc Bracoud,[6] Alison D. Murray,[2] Peter Bentham,[4] Christopher M. Kipps,[7] Charles R. Harrington[2,4] and Claude M. Wischik[2,4]

[1] Swansea University Medical School, Health Data Research UK, Swansea University, Swansea, UK.

[2]School of Medicine, Medical Sciences and Nutrition, University of Aberdeen, Aberdeen, UK

[3]Medical Physics, NHS Grampian, Aberdeen, UK

[4]TauRx Therapeutics, Aberdeen, UK

[5]School of Psychology, University of Aberdeen, Aberdeen, UK

[6]Bioclinica, Lyon, France

[7]University Hospital Southampton and University of Southampton, Southampton, UK

Correspondence to: Claude M. Wischik

TauRx Therapeutics Ltd., 395 King Street, Aberdeen AB24 5RP, United Kingdom.

E-mail: cmw@taurx.com

Running title: Core networks in behavioural variant FTD

Abstract

The behavioural variant of frontotemporal dementia is a clinical syndrome characterised by changes in behaviour, cognition and functional ability. Although atrophy in frontal and temporal regions would appear to be a defining feature, neuroimaging studies have identified volumetric differences distributed across large parts of the cortex, giving rise to a classification into distinct neuroanatomical sub-types. Here, we extended these neuroimaging studies to examine how distributed patterns of cortical atrophy map onto brain network hubs. We used baseline structural magnetic resonance imaging data collected from 213 behavioural variant of frontotemporal dementia patients meeting consensus diagnostic criteria and having definite evidence of frontal and/or temporal lobe atrophy from a global clinical trial conducted in 70 sites in Canada, United States of America, Australia, Asia and Europe. These were compared with data from 244 healthy elderly subjects from a well-characterised cohort study. We have used statistical methods of hierarchical agglomerative clustering of 68 regional cortical and subcortical volumes (34 in each hemisphere) to determine the reproducibility of previously described neuroanatomical subtypes in a global study. We have also attempted to link the structural findings to clinical features defined systematically using well-validated clinical scales (Addenbrooke's Cognitive Examination Revised, the Mini-Mental Status Examination, the Frontotemporal Dementia Rating Scale and the Functional Assessment Questionnaire) and subscales derived from them. Whilst we can confirm that the subtypes are robust, they have limited value in explaining the clinical heterogeneity of the syndrome. We have found that a common pattern of degeneration affecting a small number of subcortical, limbic and frontal nodes within highly connected networks (most previously identified as rich club members or functional binding nodes) is shared by all the anatomical subtypes. Degeneration in these core regions is correlated with cognitive and functional impairment, but less so with behavioural impairment. These findings suggest that degeneration in highly connected basal, limbic and frontal networks is a core feature of the behavioural variant of frontotemporal dementia phenotype irrespective of neuroanatomical and clinical

heterogeneity, and may underly the impairment of integration in cognition, function and behaviour responsible for the loss of insight that characterises the syndrome.

Keywords: behavioural variant frontotemporal dementia, brain networks, rich club, neurodegeneration, anatomical subtypes

Abbreviations: ABC36 = Aberdeen 1936 Birth Cohort; ACE-R = ; AD = Alzheimer's disease; bvFTD = behavioural variant of frontotemporal dementia; eTIV = estimated total intracranial volume; FAQ = functional activities questionnaire; FD = frontal-dominant; FRS = frontotemporal dementia rating scale; FTD = frontotemporal dementia; FTD = frontotemporal dementia; FTP = frontotemporoparietal; FP = frontoparietal; GLM = general linear model; MMSE = mini-mental state examination; MNI = Montreal Neurological Institute; ROI = region of interest; SL = sub-lobar; TD = temporal-dominant; VBM = voxel-based morphometric.

Introduction

Frontotemporal dementia (FTD) is a heterogeneous disorder with distinct clinical phenotypes associated with multiple neuropathologic entities (Olney *et al.,*, 2017). The core FTD disorders are behavioural variant frontotemporal dementia (bvFTD), semantic variant primary progressive aphasia, and non-fluent variant primary progressive aphasia, but there are other disorders within the FTD spectrum that include frontotemporal dementia with motor neurone disease, progressive supranuclear palsy and corticobasal syndrome. Most cases of FTD have underlying tau, transactive response DNA-binding protein-43 (TDP-43) or fused in sarcoma, Ewing's sarcoma or TATA-binding protein associated factor 15 (collectively known as the FET protein family) neuropathology (Mackenzie and Neumann 2016).

bvFTD is a clinical syndrome characterised by insidious onset and progressive deterioration in behaviour, cognition and functional ability, the core symptoms being: disinhibition, apathy, lack of empathy, compulsions, hyperorality and impairment of executive function (Rascovsky *et al.,*, 2011). Recently, higher levels of socially inappropriate behaviour and criminality in bvFTD compared with Alzheimer's disease (Liljegren *et al.,*, 2019) have been recognised, due to a dissociation between factual and evaluative understanding of actions and their consequences (Mendez, 2010; Sfera *et al.,*, 2014). Some patients may display the core clinical symptoms as a phenocopy syndrome that is not associated with brain atrophy (Devenney *et al.,,* 2018; Kipps *et al.,*. 2009; Valente *et al.,*, 2019). The revised diagnostic criteria for bvFTD therefore additionally require imaging evidence of a frontotemporal abnormality for a diagnosis of probable bvFTD.

Although atrophy in frontal and temporal regions would appear to be a defining feature, neuroimaging studies have identified volumetric differences distributed across large parts of the cortex, giving rise to a classification into distinct neuroanatomical sub-types (Josephs *et al.,* 2009; Ranasinghe *et al.,* 2016; Rohrer *et al.,* 2011; Whitwell *et al.,* 2009, 2013). Different patterns of atrophy have also been associated with different types of FTD pathology and mutations (Perry *et al.,* 2017; Rohrer *et al.,* 2009). However, all pathological subgroups appear to share atrophy in the anterior cingulate, fronto-insula

region, striatum, and amygdala. Studies of genetic frontotemporal dementia have also shown that structural brain changes occur in insula at least ten years before expected symptom onset (Rohrer *et al.,* 2015). These vulnerable connected regions, which are affected early in bvFTD, are part of what has been termed the 'salience' network which is thought to be responsible for processing of behaviourally salient stimuli in the normal brain (Perry *et al.,* 2017; Seeley, Menon, *et al.,* 2007; Seeley *et al.,* 2008, 2009). However, resting state network functional abnormalities may also extend to the default mode, fronto-parietal and semantic appraisal networks resulting in other symptoms affecting attention, working memory and semantics (Filippi *et al.,* 2013; Ranasinghe *et al.,* 2016). Recent evidence shows that the overlapping regions of resting state networks are organised into highly interconnected brain network hubs. Brain hubs are implicated in many types of dementia because of the role they play in integrating brain functions (van den Heuvel & Sporns, 2013). Given the highly heterogeneous neuroanatomical sub-types in bvFTD, it is interesting to ask whether the anatomical heterogeneity involves these central brain regions, or whether atrophy in core regions is a common feature independent of cortical heterogeneity. We have previously reported the results of a voxel-based morphometric (VBM) comparison of baseline MRI scans of patients in a large randomised controlled clinical trial in bvFTD (TRx-237-007, NCT01626378) with those randomised to a comparable study of mild AD (TRx-237-005). This showed that the bvFTD group was clearly distinguishable from the mild AD group with a similar overall level of cognitive impairment (Shiells *et al.,* 2020; Vuksanović *et al.,* 2019). As expected, the bvFTD patients had significantly more atrophy in frontal cortex and anterior temporal cortex, and significantly less atrophy in hippocampus, middle temporal gyrus, cuneus and insula.

We undertook the present study to determine how the apparent cortical heterogeneity of bvFTD subtypes relates to atrophy in central brain hubs and whether the subtypes are associated with distinctive clinical profiles. To address these question, we have used baseline structural magnetic resonance imaging (MRI) data collected from 213 bvFTD patients meeting consensus diagnostic criteria (Rascovsky *et al.,* 2011) and having definite evidence of frontal and/or temporal lobe atrophy (Kipps *et al.,* 2008) and compared this with data from 244 healthy elderly subjects from a well-characterised cohort study (Murray *et al.,* 2011). In addition, the availability of systematically collected clinical baseline scores

using validated cognitive and functional scales provided the opportunity to determine how neuroanatomical subtypes and atrophy in brain networks relate to distinctive clinical profiles. Whilst we confirm the existence of the subtypes, we show that they have limited ability to explain clinical heterogeneity in bvFTD. On the other hand, we report that the subtypes share a common pattern of degeneration affecting a small number of highly connected nodes which have a subcortical, limbic and frontal distribution. Degeneration in these nodes is highly correlated with cognitive and functional impairment irrespective of subtype.

Methods

Study participants

Study TRx-237-007 was designed as a 52-week Phase three, randomised, controlled, double-blind, parallel-group trial conducted at 70 sites in Canada, United States of America, Australia, Asia and Europe. Eligible patients had to be younger than 80 years of age with a diagnosis of bvFTD according to criteria revised by the International bvFTD Criteria Consortium (Rascovsky *et al.,* 2011), with mini-mental status examination (MMSE; (Folstein *et al.,* 1975)) score greater than or equal to 20 at screening. There was an additional requirement that patients had to meet the criterion of having definite brain atrophy in frontal and/or temporal lobes scoring two or more on a scale proposed by Kipps (Kipps *et al.,* 2008). Concomitant use of acetylcholinesterase inhibitors or memantine (or both) was permitted provided this was at a stable dose for at least 18 weeks before randomisation. Concomitant use of serotonergic antidepressant, antipsychotic (except clozapine or olanzapine) and sedative medications was also permitted at stable doses where clinically feasible. Each patient had one or more study partners participate with them in the trial as informants. Patients were excluded from the study if they had a significant CNS disorder other than bvFTD. A detailed list of inclusion and exclusion criteria in the protocol is available in the Supplementary Materials in Shiells *et al.* (Shiells *et al.,* 2020). As reported in that paper, the mean (SD) time since diagnosis of bvFTD was 1.9 (2.4) years, the MMSE severity at baseline was 24.6 (3.1) and 82.3% of the cases were at Kipps MRI severity stages 2 or 3. Of the 7/159 cases in whom mutations in coding regions were

identified, 6 involved the tau gene and one implicated TDP-43. Baseline MRI scans were evaluated by a single independent neuroradiologist out of a pool of trained neuroradiologists to determine eligibility (RadMD, NY).

In addition, MRI scans were obtained from 244 age-matched healthy controls from the well characterised Aberdeen 1936 Birth Cohort (ABC36) brain imaging database held in the Aberdeen Biomedical Imaging Centre at the University of Aberdeen. The ABC36 project has been described elsewhere (Murray *et al.,* 2011; Whalley *et al.,* 2011). Demographics and clinical characteristics of the study groups are given in Table 1.

MRI data collection

The acquisition protocol was standardised across sites using 1.5T and 3T scanners manufactured by General Electric, Philips or Siemens. All data were centrally collected, quality-controlled and analysed by the imaging core laboratory (Bioclinica). MRI data acquisition included a 3D sagittal T1-weighted sequence which we used in our analysis here. 3DT1 images were acquired using a 3D MPRAGE sequence (Siemens) or the specific manufacturer equivalent sequence (General Electric 3D IR-prepped Fast SPGR, Philips 3D TFE), covering the whole brain with a resolution of $1.25\times1.25\times1.2$ mm^3.

FreeSurfer version 5.3.0 (http://freesurfer.net/) was used to extract regional volumes for the clustering analysis. FreeSurfer automated segmentation parcelates the brain into 76 regions according to the Desikan-Killiany Atlas (Desikan *et al.,* 2006). For the purpose of this study, we selected 68 regional volumes (34 from each hemisphere) of the frontal, temporal or parietal lobe and additional sub-lobar regions (limbic lobes, basal ganglia, amygdala and thalamus) previously identified as locations of atrophy in bvFTD and/or as anatomical correlates of clinical symptoms. A full list of regions is given in the Supplementary Table 1.

Hierarchical agglomerative clustering, implemented in SPSS v.23.0, was used to classify differences/similarities in the 68 regional volumes. The bottom-up hierarchical agglomerative clustering is based on similarities and linkages between data points (subject-wise region of interest [ROI] volumes on MRI), with successive agglomeration of pairs of clusters until all clusters are merged into a single cluster containing all subjects. Similarity

was measured by Euclidean distance between pairs of data points and linkage was measured by Ward's linkage method (Ward, 1963). It is possible to classify bvFTD groups into either three or four clusters depending on the cluster distance. We used the 4-group clustering in further analyses for consistency with previous studies (Ranasinghe *et al.,* 2016; Whitwell *et al.,* 2009). Each of these groups was compared to the healthy elderly subject group using voxel based morphometry (VBM).

The VBM processing procedure employed for this study followed the steps described in by Ashburner (Ashburner, 2015). In short, the images were first segmented into grey matter, white matter and cerebrospinal fluid mask images (Ashburner, 2015; Ashburner and Friston, 2005). Each class of the segmented images were then warped together and non-linearly registered so that they matched each other (Ashburner and Friston, 2011). A custom template was created from a data set of all participants in the study. Finally, images were normalized to the Montreal Neurological Institute (MNI) space and smoothed with a Gaussian kernel (8 mm FWHM). Each group identified by the clustering technique was compared to the healthy control group. Regions showing atrophy in the bvFTD group were identified from the MNI coordinates of the voxels within the areas that were significantly different using maximum difference t-test statistics. All image processing steps and statistical analysis were implemented in the Statistical Parametric Mapping (SPM12) software package available at http://www.fil.ion.ucl.ac.uk/spm/. The t-tests were performed on each pair of voxels/volumes corrected for age, gender and either estimated total intracranial volume (Whitwell *et al.,* 2009) or total brain volume (Bigler and Tate, 2001) to correct for global atrophy/severity. Recording sites were included in the model as a random covariate. To correct for the false discoveries of significant differences due to multiple tests, the t-test statistics were corrected at the significance level $p < 0.05$ using the family-wise-error correction available in the VBM statistical package. Figure 1 shows overall procedure: generation of 68 regions of interest (ROIs) in Free Surfer, classification of bvFTD subjects into four clusters using hierarchical clustering and cluster-wise comparisons with healthy control using VBM to determine regions affected by neurodegeneration.

Clinical assessments

Baseline clinical assessments included the Addenbrooke's Cognitive Examination Revised (ACE-R) (Mioshi *et al.,* 2006), the Mini-Mental State Examination (Folstein *et al.,* 1975), the Frontotemporal Dementia Rating Scale (FRS) (Mioshi *et al.,* 2010) and the Functional Assessment Questionnaire (FAQ)(Pfeffer *et al.,* 1982). The bvFTD subtypes were compared using these scales and using subscales derived from the ACE-R and FRS prior to identification of the bvFTD subtypes. A total of 18 subscales were created: 11 cognitive subscales (from the ACE-R) and seven behavioural subscales (from the FRS). The FAQ scale was used in its entirety as an independent measure of activities of daily living. The primary scales and derived subscales are described in greater detail in the Supplementary Information.

Statistical analyses

Statistical analyses were performed using SPSS v.23.0, employing paired samples t-tests to compare males and females in Table 1. One-way ANOVA was used to test differences between bvFTD subtypes in cognitive and behavioural sub-scores given in Table 2. A significance level of $p < 0.05$ was used.

In order to generate a summary variable accounting for the multiple regional volumes affected by neurodegeneration, we employed a post hoc principal component analysis to reduce the volume measurements into a manageable number of factors. We examined clinical-anatomical correlations using general linear models (GLM). In these we tested for associations between clinical measures and the first volumetric summary variable accounting for 40% of the variance. The models used included adjustments for known and potential confounders: age, sex, head size and anatomical subtype.

Data Availability

Data supporting the findings of this study are available from the corresponding author, upon reasonable request.

Results

Demographic and clinical features of the populations studied

A total of 213 bvFTD patients of 220 randomised to the trial were included in the present study based on baseline MRI scan quality and the complete clinical data required for the present study at baseline. Baseline demographic and clinical data are provided in Table 1. Mean (± SD) age was 63 ± 7 years for both males (136) and females (77). Total years in education were 15.4 ± 0.5, with no difference between males and females. The estimated total intracranial volume (eTIV) was significantly larger in males (1600 ± 220 cm^3) than in females (1400 ± 150 cm^3), although there was no difference in brain parenchymal fraction (BF, 0.67 ± 0.06). The MMSE score was significantly higher in males (25.4 ± 3.5) than in females (22.9 ± 4.0), as was the total ACE-R score (males: 72 ± 16; females: 62 ± 14). Males performed better on most of the ACE-R subscales apart from phonemics, language structure, episodic memory and perceptual abilities. By contrast, there was no overall difference on either the FRS or the FAQ score between males and females. The only FRS subscales showing a gender difference were ADL (where males performed better) and disinhibition (where males performed worse). There were no demographic differences between patients prescribed symptomatic treatments approved for AD (but not bvFTD) and those not receiving these treatments.

There were 133 males and 111 females in the healthy elderly group. There were no sex differences in age, years of education or MMSE score. The healthy elderly group was significantly older (69 ± 2 years), had less education (11 ± 2 years), and had a higher MMSE score (28.9 ± 1.2) than the bvFTD group.

Classification of bvFTD subjects by agglomerative clustering based on regional brain volumes

We applied a hierarchical agglomerative clustering algorithm using Euclidean distance and Ward linkage to provide measures of differences/similarities in the 68 regional volumes of the Desikan-Killiany Atlas (Desikan *et al.,* 2006). The tree/dendrogram is shown in Supplementary Fig. 1. It is possible to classify bvFTD groups into either three or four clusters depending on the cluster distance. We used the 4-group clustering in further

analyses for consistency with previous studies (Ranasinghe *et al.,* 2016; Whitwell *et al.,* 2009). Each of these groups was then treated as a single group and compared to the healthy elderly subject group using VBM. Figure 2 shows the 3D surface rendering of the voxel-wise differences between each of the bvFTD groups and the healthy elderly group after correction for total intra-cranial volume. A similar result was found when the correction was based on estimated brain volume (Supplementary Fig. 3). Following Whitwell and colleagues (Whitwell *et al.,* 2013), we designated the four anatomical sub-types: fronto/temporo/parietal (FTP), frontal-dominant (FD), temporal-dominant (TD) and sub-lobar (SL). The differences in cortical atrophy across bvFTD subtypes are shown in Figure 3.

Degeneration of central basal and limbic nodes as a core feature of bvFTD

Having confirmed the classification of the bvFTD subtypes based on distinct patterns of cortical atrophy, we determined how these are linked to atrophy in subcortical and limbic regions (Supplementary Fig. 3 and Table 2). As shown in Tables 2 and 3, we found that it is possible to distinguish regions that are common to the four subtypes from those that are not. The limbic structures found to be common to all subtypes in terms of atrophy included anterior cingulate gyrus, hippocampal and parahippocampal gyri, insula and temporal pole (superior temporal gyrus). The subcortical grey nuclei affected in all subtypes included amygdala, caudate nucleus, pallidum and thalamus. The cortical regions common to the subtypes were the orbital surface areas of the frontal cortex (inferior frontal gyrus, olfactory cortex and gyrus rectus) and the medial surface areas of the frontal cortex (superior frontal gyrus and supplementary motor area). Only the middle temporal gyrus of the temporal lobe was shared between the subtypes. In all cases, the involvement of the common regions was bilateral.

A striking feature of the regions of atrophy shared across subtypes was that all have been identified previously as either members of the rich club (van den Heuvel *et al.,* 2012) or functional binding nodes (Deco *et al.,* 2017), or as regions having higher than average connectivity. As shown in Supplementary Fig. 3 and in Table 2, the rich club members identified as undergoing atrophy in all four bvFTD sub-types were superior frontal gyrus, thalamus, pallidum, putamen and hippocampus. The functional 'binding' regions (Deco *et*

al., 2017) common to the four subtypes include anterior cingulate and insula. In addition, parahippocampal gyrus, amygdala and caudate have been identified as highly connected nodes.

By contrast with these subtype-independent regions, the regions listed in Table 3 had more limited subtype overlap and were generally unilateral. Atrophy in the superior temporal gyrus was unique to the TD subtype. The FTP subtype showed atrophy in middle occipital gyrus and precuneus, and the latter is also seen in the FT subtype. There was no overlap between atrophy and any of the rich club or linker regions that was unique to the SL subtype. Degeneration in the superior occipital lobe was unique to the frontal-dominant subtype. Atrophy in the superior temporal gyrus, although a functional binding node, was unique to the temporal-dominant subtype.

Cognitive, functional and behavioural performance across bvFTD subtypes

The principal cognitive scales, ACE-R and MMSE, showed no significant differences according to the bvFTD subtypes (Table 4). By contrast, the functional and behavioural scales, FAQ and FRS, showed significant differences (Table 4 and Figure 4), with the FD subtype showing greater overall impairment than the others. To examine this further, we used FRS subscales to determine whether behavioural elements of the bvFTD syndrome could be differentiated according to subtype. As shown in Table 4 and Figure 4, a picture like that seen with the full scales emerged, namely that the FD subtype was generally more impaired than the others. This could be seen for behavioural symptoms (characterised predominantly by lack of appropriate behaviours), apathy/disinterest and disinhibition. The only significant exception was that both the FD and TD subtypes were characterised by significantly greater impairment on the subscales measuring problematic behaviours than the FTL and SL subtypes. Although it was possible to map functional and behavioural deficits to specific cortical regions (Supplementary Figs. 7 and 8), these features did not discriminate between the bvFTD subtypes identified by structural criteria, apart from greater general impairment largely restricted to the FD subtype (see also Supplementary Fig. 7).

Since overall cognitive impairment did not provide a basis for discriminating between the subtypes, we next tested whether cognitive subdomains possessed greater discriminatory capacity. Here a more complex picture emerged, as shown in Table 4 and Figure 5 (and Supplementary Fig. 8). As expected, the TD subtype was characterised more specifically by greater impairment in semantic memory and language semantics, but not in episodic memory. The FD subtype was differentiated by more prominent deficits in letter fluency. The FTP subtype showed somewhat greater impairment in language phonemics and perceptual abilities. There were no cognitive deficits that could be linked more specifically to the SL subtype. Although the FTD subtype might appear to be more AD-like, there were no differences in likelihood of being prescribed symptomatic treatments approved for AD.

A post-hoc examination of the relationship between anatomical core features and cognitive, behaviour and functional performance in bvFTD.

It is clear from the foregoing analysis that atrophy patterns in bvFTD can be split into those atrophy patterns which are common to all subtypes and those that are associated with specific subtypes. Using the core regions, we performed a principal components data reduction and found that the first unrotated factor explained 40% of the variance found across all core regions. There were significant correlations between this extracted factor and cognitive, behaviour and functional scores (Table 5). We next used a general linear model (GLM) approach to determine whether these associations depend on unique features of the subtype. In this analysis, the cognitive, behaviour and functional scores were considered separately as the dependent variable, and sex and subtype were included as fixed factors, while age, the summary core factor and head size were included as covariates (Table 5). The GLM analysis showed that the summary core feature drives the association with the cognitive scores and the functional activity score. By contrast, the behavioural score is associated with the cortical subtype, but not with the summary core feature.

Discussion

We have analysed a large clinical cohort of 213 well characterised bvFTD patients from a global, multicentre study. We aimed to examine how common and heterogeneous patterns of atrophy account for clinical diversity in this syndrome. Whilst confirming the existence of four anatomically distinct subtypes at the cortical level, our study has identified sub-lobar and limbic brain atrophy as a core feature of bvFTD that is common to the anatomically distinct subtypes that have been described. A summary metric based on core region atrophy was found to associate significantly with cognitive and functional performance across all subtypes. Conversely, cortical heterogeneity was associated with behavioural performance independent of the variance explained by the core features. Therefore, the bvFTD syndrome can be understood as comprising a core disturbance in highly connected subcortical and limbic brain structures that is closely linked to cognitive and functional impairment.

Common and distinct atrophy patterns

Despite the existence of four anatomically distinct patterns of cortical surface atrophy in the population we have analysed, there is a homogenous pattern of atrophy across sub-cortical and limbic regions that is common to the anatomical subtypes. Of 39 brain regions showing atrophy when compared to heathy elderly subjects, 16 regions were found to be common to all four subtypes, whereas 23 had selective subtype associations. Of the 16 subtype-independent regions of atrophy, 10 have been characterised previously as brain hubs, i.e., brain regions with higher than average connectivity. These 10 regions map either to the so-called "rich club" of highly connected nodes (van den Heuvel *et al.,* 2012), to highly connected functional binding nodes (Deco *et al.,* 2017) or nodes known to have higher than average connectivity in either functional or structural MRI studies (Robinson *et al.,* 2012; Ward *et al.,* 2014). These network hubs are central to communication and functional integration of the brain and represent potential hotspots for loss of connectivity across multiple brain networks (Gollo *et al.,* 2015). It is known from previous studies that the sub-networks of highly connected nodes play an important role in efficient information processing between segregated brain areas (Bullmore and Sporns, 2012) and have been found to be associated with cognitive performance (Baggio *et al.,* 2015) in healthy brain.

Meta-analysis of MRI studies has suggested that the structural brain hubs and their connections are highly vulnerable to neurodegeneration (Crossley *et al.,* 2014; Sha *et al.,* 2018) although the hubs implicated in bvFTD and AD differ (Daianu *et al.,* 2016). Of the 23 regions where atrophy is not shared across the subtypes, two were found to be either subcortical or limbic, and five are members of the rich club or functional binding group. We therefore conclude that degeneration in basal, limbic and frontal networks that have high levels of connectivity represents a core feature of the bvFTD syndrome irrespective of the distinct cortical subtypes that have been described.

Degeneration of brain network hubs is not unique to bvFTD. It has been noted that neurodegeneration targets brain hubs in most of the neurodegenerative disorders (van den Heuvel and Sporns, 2019; Stam, 2014; Stam and van Straaten, 2012). As noted above, the anatomical sites of atrophy differ between different neurodegenerative disorders. For example, the central brain regions affected in AD are more likely to be the medial temporal and parietal regions, although thalamus and hippocampus are consistently atrophied in both bvFTD and AD. It has been proposed that the increased traffic that hubs are required to support may help to explain why these regions have preferentially greater vulnerability to neurological disorders in general (van den Heuvel and Sporns, 2013*a*; de Lange *et al.,* 2019; Stam, 2014). The vulnerability of the central networks of the human brain to neurodegeneration (Stam, 2014) may explain the involvement of some rich club network nodes (insula, anterior cingulate, hippocampus, superior temporal pole, pallidum and thalamus), but not all (putamen and a number of cortical regions). A high degree of connectivity may also make certain regions more vulnerable to prion-like spread of pathology arising stochastically in linked subregions. These need not be mutually exclusive, since a chronically high level of activity may itself lead to high demands on turnover of vulnerable protein systems and predispose to pathological aggregation and transmission.

The core regions identified in this study underpin brain functions relevant to the core clinical diagnostic symptoms of bvFTD. The superior frontal gyrus is involved in self-awareness, cognitive control, emotion regulation, and impulse control. Reduced volumes in FTD have been associated with disinhibition (Cajanus et al., 2019) and ADL dysfunction (Mioshi et al.,2013). Striatal damage is strongly linked with executive dysfunction,

impaired reward-punishment processing, and affective and motivational disturbances (O'Callaghan et al., 2014). Striatal atrophy occurs early in bvFTD and has also been associated with eating changes. The von Economo neurons (VENs) of the anterior cingulate cortex, important for empathy, social awareness, and self-control, are severely depleted early in bvFTD (Allman et al., 2010). VENs from the anterior insula are thought important for awareness and together form a network with the striatum and amygdala. The amygdala plays a prominent role in mediating decision making, emotional learning and behaviour and is often affected early in bvFTD, particularly in cases due to MAPT mutations (Bocchetta et al., 2019). The thalamus is a complex modulatory gate. The anteroventral and dorsomedial nuclei form part of the dorsolateral prefrontal circuit, related to executive function and motor programming, and are also part of the lateral orbitofrontal circuit, related to personality and mood regulation (Bocchetta et al., 2018). Thalamic atrophy is particularly prominent with TDP-43 pathology and C9orf72 mutations (Bocchetta et al., 2018).

In an admittedly simplified model, Seeley and colleagues have proposed that neurodegeneration in bvFTD targets primarily the salience network (Seeley *et al.* 2012). It is hypothesised that this would be responsible for social-emotional-autonomic processing (Seeley, Allman, *et al.,* 2007) and affect some other functional brain networks via its afferent/efferent interactions. The salience network is closely allied with the ventral valuation/context appraisal network also known as the semantic appraisal network (Guo *et al.,* 2013), default mode network and task-control or executive network (Cole and Schneider, 2007; Possin *et al.,* 2013), all reported as being disrupted in bvFTD. The trans-modal areas of the default mode and salience network also overlap with the rich club network regions (van den Heuvel and Sporns, 2013*b*; Uddin *et al.,* 2011). Our results support the existence of a common underlying pattern of degeneration which is not restricted to the salience network. Different cortical subtypes of bvFTD ranging from absence of cortical lobar atrophy, to lobe-specific dominance, to multi-lobar atrophy, all share degeneration in the basal, limbic and frontal networks we have described.

In our cohort, the fronto-temporo-parietal subtype had the highest frequency (39%) and the frontal-dominant (19%), the temporal-dominant (24%) and the sub-lobar subtypes (18%) had comparable lower frequencies. Therefore, the syndrome as defined by

consensus clinical criteria and by the requirement for a significant degree of frontal and/or temporal lobe atrophy remains neuroanatomically heterogeneous in the population we have studied. Our results align with two smaller studies reporting consistent differences in patterns of degeneration across cortical areas in patients diagnosed as having bvFTD by consensus criteria (Ranasinghe *et al.,* 2016; Whitwell *et al.,* 2009). This consistency between studies is preserved despite sampling of different subsets of regional volumes and utilisation of different statistical classifications. The frontal-dominant, temporal-dominant and fronto-temporo-parietal groups are comparable with the same anatomical sub-types identified by Whitwell and colleagues (2009). Ranasinghe and colleagues (2016) designate essentially the same anatomical subtypes in terms of a theoretical construct as the salience-network-frontal subtype (i.e., frontal-dominant), the semantic appraisal-network sub-type (i.e., temporal dominant) and salience-network-frontotemporal (i.e., fronto-temporo-parietal) subtype. Their sub-cortical subtype parallels our sub-lobar subtype. Although it is possible that the sub-lobar subtype might represent an earlier stage of the disease, Ranasinghe and colleagues have argued that it represents a true bvFTD subtype which progresses more slowly. We found no global cognitive, functional or behaviour differences which might have been expected if it represented an earlier stage of the disease. Our data therefore support the suggestion of Ranasinghe and colleagues that this is indeed a distinct subtype, and that its prevalence is comparable to that of the frontal- and temporal-dominant subtypes.

Heterogeneity at the cortical level is associated to only a limited extent with distinct behavioural, functional and cognitive features. The frontal-dominant subtype is characterised by greater global impairment on both the FRS and FAQ scales. It is notable that the frontal-dominant subtype is the most severely affected in terms of behavioural symptoms such as lack of appropriate social response, apathy and disinterest, as well as disinhibition and problematic positive behaviours. In other words, in contrast to the overall importance of highly connected networks in defining the bvFTD syndrome, the frontal lobe remains particularly important for regulation of behaviour. By contrast, cognitive deficits segregate as expected, with the temporal-dominant form associated particularly with semantic memory and language semantics, and a stronger association between frontal-dominant atrophy and impairment in letter fluency.

Independently of the sub-type, a summary metric variable for the core features (the first unrotated factor), was found to have a highly significant statistical association with cognitive impairment, particularly with ACE-R, and with functional impairment as measured by the FAQ scale. After adjusting for the core factor, there was no residual association with subtype. On the other hand, the behavioural subscale derived from the FRS retained a significant association with anatomical subtype after taking account of the core factor variable. This may explain the possible latent nature of the pure sub-lobar subtype (Ranasinghe *et al.,* 2016) in which prominent behavioural deficits may not be demonstrated.

This mapping of imaging features to clinical features should be viewed in the context of the inclusion criteria of this study, namely the requirement for presence of brain atrophy in frontal and/or temporal lobes scoring two or more on a scale proposed by Kipps (Kipps *et al.,* 2008). That is subjects with little or no frontal and/or temporal atrophy and who fulfilled all other criteria for bvFTD were not included. The results of the present analysis suggest that the diagnostic utility of MRI in the differentiation of bvFTD from healthy controls and other dementias may be best served by examining the core features with or without the frontal and temporal lobes. A recent study reports that a data driven approach for discriminating between bvFTD patients and controls showed good discriminatory performance without a priori knowledge of any potential structure within the data (Manera *et al.,* 2019). It remains to be determined how a prior knowledge of the core features we have described could improve the discrimination. More importantly, it remains to be determined how incorporating a core feature metric assists with the more pertinent clinical question which is to discriminate between bvFTD and other dementias.

Limitations and conclusions

There are limitations to the inferences which can be drawn from the present study. Although it is based on a large sample, it is possible that still greater power is required to define the subtle clinical features of the subtypes. Similarly, the clinical scales we have used to interrogate the bvFTD phenotype may not be sufficiently discriminatory, and more refined neuropsychological measures may characterise the clinical features of the subtypes with greater subtlety. A further limitation is that we have used patterns of atrophy on MRI

as the sole investigative tool for analysing the brain abnormalities of bvFTD. Although this has the advantages of a wide applicability and standardisation, metrics based on functional MRI that may be able to define abnormalities in the underlying connectome were not available in the present study. Again, there is a trade-off between the feasibility of more refined approaches and study size/cost considerations.

Notwithstanding these limitations, a useful general picture that emerges from our study is that the MRI abnormalities in the bvFTD syndrome can be characterised at two neuroanatomical levels. The core of the syndrome appears to depend on a common pattern of degeneration in which basal and limbic lobes are disproportionately represented. Some, but not all of these, have been identified previously as brain structural and functional network hubs. In addition, the neuroanatomical heterogeneity at the cortical level, which is robust and reproducible across studies, appears to have limited explanatory power in accounting for cognitive, functional and behavioural heterogeneity. Our results are consistent with the idea that bvFTD is characterised by a core disturbance within basal, limbic and frontal networks required for integration of cognition, function and behaviour. This core disturbance at the level of integration may help to understand both the inappropriate conduct that families find distressing and the higher rates of socially inappropriate behaviour and criminality in bvFTD than in other comparable neurodegenerative disorders (Liljegren *et al.,* 2019). There appears to be a dissociation between the cognitive understanding of actions and their consequences as matters of fact, and the capacity for an appropriate evaluation of their personal and societal implications (Mendez, 2010; Sfera *et al.,* 2014). The loss of insight that characterises the condition could be understood as resulting from pathology affecting particularly the central integrative systems that enable segregated functional regions of the brain to interact and communicate.

Acknowledgments

We would like to acknowledge the support of the Maxwell Computer Cluster at the University of Aberdeen. We also gratefully acknowledge study investigators and the generosity of study participants.

Funding

This study was sponsored entirely by TauRx Therapeutics Ltd. (PAR1577). The Maxwell Computer Cluster is funded by the University of Aberdeen. Supplementary material

Supplementary material is available at Brain Communication online.

Competing Interests

The sponsor was involved in the design of the study; in the collection, analysis and interpretation of data; and in the writing of the report. The corresponding author had full access to all the data and had final responsibility for submission of the report for publication. All authors approved the final submission. CRH and CMW are employees and officers of TauRx Therapeutics Ltd. SM and PB are employees of TauRx. VV, RTS, SM, ADM, CRH and CMW are inventors on patents relating to imaging in neurodegenerative diseases that are owned by WisTa Laboratories Ltd., an affiliate of TauRx Therapeutics Ltd.

References

Ashburner J. VBM Tutorial. Univ Coll London 2015 [accessed from www.fil.ion.ucl.ac.uk/~john/misc/VBMclass15.pdf].

Ashburner J, Friston KJ. Unified segmentation. Neuroimage 2005; 26: 839–51.

Ashburner J, Friston KJ. Diffeomorphic registration using geodesic shooting and Gauss–Newton optimisation. Neuroimage 2011; 55: 954–67.

Baggio HC, Segura B, Junque C, de Reus MA, Sala-Llonch R, Van den Heuvel MP. Rich Club Organization and Cognitive Performance in Healthy Older Participants. J Cogn Neurosci 2015; 27: 1801–10.

Bigler ED, Tate DF. Brain Volume, Intracranial Volume, and Dementia. Invest Radiol 2001; 36: 539–46.

Bullmore E, Sporns O. The economy of brain network organization. Nat Rev Neurosci 2012; 13: 336–9.

Cole MW, Schneider W. The cognitive control network: Integrated cortical regions with dissociable functions. Neuroimage 2007; 37: 343–60.

Crossley NA, Mechelli A, Scott J, Carletti F, Fox PT, McGuire P, et al. The hubs of the human connectome are generally implicated in the anatomy of brain disorders. Brain 2014; 137: 2382–95.

Daianu M, Mezher A, Mendez MF, Jahanshad N, Jimenez EE, Thompson PM. Disrupted rich club network in behavioral variant frontotemporal dementia and early-onset Alzheimer's disease. Hum Brain Mapp 2016; 37: 868–83.

Deco G, Van Hartevelt TJ, Fernandes HM, Stevner A, Kringelbach ML. The most relevant human brain regions for functional connectivity: Evidence for a dynamical workspace of binding nodes from whole-brain computational modelling. Neuroimage 2017; 146: 197–210.

de Lange SC, Scholtens LH; Alzheimer's Disease Neuroimaging Initiative, et al. Shared vulnerability for connectome alterations across psychiatric and neurological brain disorders. Nat Hum Behav 2019; 3: 988-98.

Desikan RS, Ségonne F, Fischl B, Quinn BT, Dickerson BC, Blacker D, et al. An automated labeling system for subdividing the human cerebral cortex on MRI scans into gyral based regions of interest. Neuroimage 2006; 31: 968–80.

Devenney E, Swinn T, Mioshi E, Hornberger M, Dawson KE, Mead S, et al. The behavioural variant frontotemporal dementia phenocopy syndrome is a distinct entity - evidence from a longitudinal study. BMC Neurol 2018; 18: 56.

Filippi M, Agosta F, Scola E, Canu E, Magnani G, Marcone A, et al. Functional network connectivity in the behavioral variant of frontotemporal dementia. Cortex 2013; 49: 2389–401.

Folstein MF, Folstein SE, McHugh PR. "Mini-mental state". J Psychiatr Res 1975; 12: 189–98.

Gollo LL, Zalesky A, Hutchison RM, van den Heuvel M, Breakspear M. Dwelling quietly in the rich club: brain network determinants of slow cortical fluctuations. Phil Trans R

Soc B Biol Sci 2015; 370: 20140165.

Guo CC, Gorno-Tempini ML, Gesierich B, Henry M, Trujillo A, Shany-Ur T, et al. Anterior temporal lobe degeneration produces widespread network-driven dysfunction. Brain 2013; 136: 2979–91.

Josephs KA, Whitwell JL, Knopman DS, Boeve BF, Vemuri P, Senjem ML, et al. Two distinct subtypes of right temporal variant frontotemporal dementia. Neurology 2009; 73: 1443–50.

Kipps CM, Hodges JR, Fryer TD, Nestor PJ. Combined magnetic resonance imaging and positron emission tomography brain imaging in behavioural variant frontotemporal degeneration: refining the clinical phenotype. Brain 2009; 132: 2566–78.

Kipps CM, Nestor PJ, Dawson CE, Mitchell J, Hodges JR. Measuring progression in frontotemporal dementia. Neurology 2008; 70: 2046–52.

Liljegren M, Landqvist Waldö M, Frizell Santillo A, Ullén S, Rydbeck R, Miller B, et al. Association of neuropathologically confirmed frontotemporal dementia and Alzheimer disease with criminal and socially inappropriate behavior in a Swedish cohort. JAMA Network Open 2019; 2: e190261.

Mackenzie IRA, Neumann M. Molecular neuropathology of frontotemporal dementia: insights into disease mechanisms from postmortem studies. J Neurochem 2016; 138: 54–70.

Manera AL, Dadar M, Collins DL, Ducharme S. Deformation based morphometry study of longitudinal MRI changes in behavioral variant frontotemporal dementia. NeuroImage Clin 2019; 24: 102079.

Mendez MF. The unique predisposition to criminal violations in frontotemporal dementia. J Am Acad Psychiatry Law 2010; 38: 318–23.

Mioshi E, Dawson K, Mitchell J, Arnold R, Hodges JR. The Addenbrooke's Cognitive Examination Revised (ACE-R): a brief cognitive test battery for dementia screening. Int J Geriatr Psychiatry 2006; 21: 1078–85.

Mioshi E, Hsieh S, Savage S, Hornberger M, Hodges JR. Clinical staging and disease progression in frontotemporal dementia. Neurology 2010; 74: 1591–7.

Murray AD, Staff RT, McNeil CJ, Salarirad S, Ahearn TS, Mustafa N, et al. The balance between cognitive reserve and brain imaging biomarkers of cerebrovascular and Alzheimer's diseases. Brain 2011; 134: 3687–96.

Olney NT, Spina S, Miller BL. Frontotemporal dementia. Neurol Clin 2017; 35: 339–74.

Perry DC, Brown JA, Possin KL, Datta S, Trujillo A, Radke A, et al. Clinicopathological correlations in behavioural variant frontotemporal dementia. Brain 2017; 140: 3329–45.

Pfeffer RI, Kurosaki TT, Harrah CH, Chance JM, Filos S. Measurement of functional activities in older adults in the community. J Gerontol 1982; 37: 323–9.

Possin KL, Feigenbaum D, Rankin KP, Smith GE, Boxer AL, Wood K, et al. Dissociable executive functions in behavioral variant frontotemporal and Alzheimer dementias. Neurology 2013; 80: 2180–5.

Ranasinghe KG, Rankin KP, Pressman PS, Perry DC, Lobach IV., Seeley WW, et al. Distinct subtypes of behavioral variant frontotemporal dementia based on patterns of network degeneration. JAMA Neurol 2016; 73: 1078-88.

Rascovsky K, Hodges JR, Knopman D, Mendez MF, Kramer JH, Neuhaus J, et al. Sensitivity of revised diagnostic criteria for the behavioural variant of frontotemporal dementia. Brain 2011; 134: 2456–77.

Robinson JL, Laird AR, Glahn DC, Blangero J, Sanghera MK, Pessoa L, et al. The functional connectivity of the human caudate: An application of meta-analytic connectivity modeling with behavioral filtering. Neuroimage 2012; 60: 117–29.

Rohrer JD, Guerreiro R, Vandrovcova J, Uphill J, Reiman D, Beck J, et al. The heritability and genetics of frontotemporal lobar degeneration. Neurology 2009; 73: 1451–6.

Rohrer JD, Lashley T, Schott JM, Warren JE, Mead S, Isaacs AM, et al. Clinical and neuroanatomical signatures of tissue pathology in frontotemporal lobar degeneration. Brain 2011; 134: 2565–81.

Rohrer JD, Nicholas JM, Cash DM, van Swieten J, Dopper E, Jiskoot L, et al. Presymptomatic cognitive and neuroanatomical changes in genetic frontotemporal dementia in the Genetic Frontotemporal dementia Initiative (GENFI) study: a cross-sectional analysis. Lancet Neurol 2015; 14: 253–62.

Seeley WW, Allman JM, Carlin DA, Crawford RK, Macedo MN, Greicius MD, et al. Divergent social functioning in behavioral variant frontotemporal dementia and Alzheimer disease: reciprocal networks and neuronal evolution. Alzheimer Dis Assoc Disord 2007; 21: S50–7.

Seeley WW, Crawford R, Rascovsky K, Kramer JH, Weiner M, Miller BL, et al. Frontal paralimbic network atrophy in very mild behavioral variant frontotemporal dementia. Arch Neurol 2008; 65: 249–55.

Seeley WW, Crawford RK, Zhou J, Miller BL, Greicius MD. Neurodegenerative diseases target large-scale human brain networks. Neuron 2009; 62: 42–52.

Seeley WW, Menon V, Schatzberg AF, Keller J, Glover GH, Kenna H, et al. Dissociable intrinsic connectivity networks for salience processing and executive control. J Neurosci 2007; 27: 2349–56.

Seeley WW, Zhou J, Kim E-J. Frontotemporal dementia. Neurosci 2012; 18: 373–85.

Sfera A, Osorio C, Gradini R, Price A. Neurodegeneration behind bars: from molecules to jurisprudence. Front Psychiatry 2014; 5: 115.

Sha Z, Xia M, Lin Q, Cao M, Tang Y, Xu K, et al. Meta-connectomic analysis reveals commonly disrupted functional architectures in network modules and connectors across brain disorders. Cereb Cortex 2018; 28: 4179–94.

Shiells H, Schelter BO, Bentham P, Baddeley TC, Rubino CM, Ganesan H, et al. Concentration-dependent activity of hydromethylthionine on clinical decline and brain atrophy in a randomized controlled trial in behavioral variant frontotemporal dementia. J Alzheimer's Dis 2020; 75: 501–19.

Stam CJ. Modern network science of neurological disorders. Nat Rev Neurosci 2014; 15: 683–95.

Stam CJ, van Straaten ECW. The organization of physiological brain networks. Clin Neurophysiol 2012; 123: 1067–87.

Uddin LQ, Supekar KS, Ryali S, Menon V. Dynamic reconfiguration of structural and functional connectivity across core neurocognitive brain networks with development. J Neurosci 2011; 31: 18578–89.

Valente ES, Caramelli P, Gambogi LB, Mariano LI, Guimarães HC, Teixeira AL, et al. Phenocopy syndrome of behavioral variant frontotemporal dementia: a systematic review. Alzheimers Res Ther 2019; 11: 30.

van den Heuvel MP, Kahn RS, Goni J, Sporns O. High-cost, high-capacity backbone for global brain communication. Proc Natl Acad Sci 2012; 109: 11372–7.

van den Heuvel MP, Sporns O. An anatomical substrate for integration among functional networks in human cortex. J Neurosci 2013; 33: 14489–500.

van den Heuvel MP, Sporns O. Network hubs in the human brain. Trends Cogn Sci 2013; 17: 683–96.

van den Heuvel MP, Sporns O. A cross-disorder connectome landscape of brain dysconnectivity. Nat Rev Neurosci 2019; 20: 435-46.

Vuksanović V, Staff RT, Ahearn T, Murray AD, Wischik CM. Cortical thickness and surface area networks in healthy aging, Alzheimer's disease and behavioral variant fronto-temporal dementia. Int J Neural Syst 2019; 29: 1850055.

Ward AM, Schultz AP, Huijbers W, Van Dijk KRA, Hedden T, Sperling RA. The parahippocampal gyrus links the default-mode cortical network with the medial temporal lobe memory system. Hum Brain Mapp 2014; 35: 1061–73.

Ward JH. Hierarchical grouping to optimize an objective function. J Am Stat Assoc 1963; 58: 236–44.

Whalley LJ, Murray AD, Staff RT, Starr JM, Deary IJ, Fox HC, et al. How the 1932 and 1947 mental surveys of Aberdeen schoolchildren provide a framework to explore the childhood origins of late onset disease and disability. Maturitas 2011; 69: 365–72.

Whitwell JL, Przybelski SA, Weigand SD, Ivnik RJ, Vemuri P, Gunter JL, et al. Distinct anatomical subtypes of the behavioural variant of frontotemporal dementia: a cluster analysis study. Brain 2009; 132: 2932–46.

Whitwell JL, Xu J, Mandrekar J, Boeve BF, Knopman DS, Parisi JE, et al. Frontal asymmetry in behavioral variant frontotemporal dementia: clinicoimaging and pathogenetic correlates. Neurobiol Aging 2013; 34: 636–9.

Figure legends

Figure 1. Analysis pipeline. A schematic of the analysis pipeline including Free Surfer Region of Interest (ROI) analysis, hierarchical clustering and Voxel-Based Morphometry (VBM). Note the involvement of two study groups, healthy control and behavoural variant frontotemporal dementia (bvFTD), in different steps. Clasification of bvFTD subjects into four clusters was done on 68 cortical regions of interest (ROIs) extracted using Free Surfer. Each cluster was then compared with the healthy control group using VBM (blue box) and anatomical bvFTD sub-types were identified from this analysis based on cortical atrophy (yellow areas on the cortical surface). The core regions are common to all four sub-types.

Figure 2. Surface maps for four sub-types. (A) Fronto-temporo-parietal; **(B)** temporal-dominant; **(C)** frontal-dominant; and **(D)** sub-lobar. bvFTD individuals clustered based on differences in the 68 regional volumes. Yellow areas represent significant volume loss in each bvFTD cluster/sub-type (sagittal and medial views) based on pair-wise comparisons with the healthy control group.

Figure 3. Surface maps for differences between sub-types. (A) TDP > FTP; **(B)** FD > FTP; **(C)** TD > FD; **(D)** FD > TD; **(E)** FTP > SL; and **(F)** FD > SL. Pair-wise differences between the four identified bvFTD clusters/groups mapped onto the cortical surface. Hot/cold colours indicate t-test statistics used for the voxel-wise comparisons. Hot colours indicate 'more' atrophy (as indicated in each panel by an inequality sign).

Figure 4. Behavioural scores by sub-type. (A) Frontotemporal dementia rating score; **(B)** functional activities questionnaire; **(C)** behavioural symptoms; **(D)** disinhibition; **(E)** apathy/disinterest; and **(F)** problematic behaviours. Box-plots with individual data points superimposed for behavioural and functional sub-scores for bvFTD sub-types.

Figure 5. Cognitive scores by sub-type. (A) Attention; **(B)** perceptual abilities; **(C)** semantic memory; **(D)** letter fluency; **(E)** language phonemics; and **(F)** language semantics. Box-plots with individual data points superimposed for cognitive sub-scores for bvFTD sub-types.

Table 1. Demographic and clinical data on bvFTD and healthy elderly subjects.

bvFTD	All Subjects N = 213 Mean (SD)	Range	Males N = 136 Mean (SD)	Females N = 77 Mean (SD)
Age (Years)	63 (7)	42 – 70	63 (7)	63 (7)
Education (Years)	12 (4)	4 – 23	12 (3)	12 (4)
Handedness (R/L;A)	195/21;2	(R/L;A)	123/13;2	72/8;0
eTIV (cm^3)	1500 (220)	897 – 3077	1600 (220)**	1400 (150)
BF (TBV/eTIV)	0.67 (0.06)	0.37 – 0.94	0.67 (0.06)	0.68 (0.05)
MMSE (0 – 30)	24.5 (3.9)	11 – 30	25.4 (3.5)**	22.9 (4.0)
ACE-R (0 – 100)	68.5 (16.0)	17 – 99	72 (16)**	62 (14)
Attention (0 – 8)	3.9 (1.5)	0 – 8	4.4 (1.2)**	3.2 (1.7)
Orientation (0 – 10)	8.2 (1.9)	1 – 10	8.5 (1.8)**	7.7 (2.1)
Category fluency (0 – 7)	2.8 (1.9)	0 – 7	3.2 (2.0)**	1.8 (1.6)
Letter fluency (0 – 7)	2.8 (1.9)	0 – 7	3.1 (2.1)**	2.2 (1.7)
Language – phonemics (0 – 2)	1.5 (0.7)	0 – 2	1.6 (0.7)	1.4 (0.8)
Language – semantics (0 – 17)	12.7 (4.4)	1 – 28	13.2 (4.7)**	11.8 (3.8)
Language – structure (0 – 7)	6.2 (1.2)	2 – 11	6.2 (1.2)	6.0 (1.0)
Episodic memory (0 – 22)	12.8 (5.0)	0 – 22	13.3 (4.7)	12.1 (5.6)
Semantic memory (0 – 4)	2.4 (1.3)	0 – 4	2.6 (1.3)**	2.1 (1.2)
Perceptual abilities (0 – 8)	7.4 (1.2)	2 – 8	7.6 (0.9)	7.0 (1.5)
Praxis (0 – 8)	5.4 (2.3)	0 – 8	6.0 (2.0)**	2.4 (0.3)
FRS (-6.66 – 5.39)	-0.42 (1.45)	-3.80 – 5.39	-0.30 (1.4)	-0.62 (1.4)
ADL (%)	0.53 (0.25)	0 – 1	0.55 (0.26)*	0.48 (0.24)
Behavioural symptoms (%)	0.41 (0.22)	0 – 1	0.40 (0.22)	0.42 (0.23)
Cognition (%)	0.36 (0.38)	0 – 1	0.38 (0.40)	0.34 (0.37)
Apathy/disinterest (%)	0.38 (0.26)	0 – 1	0.39 (0.25)	0.37 (0.28)
Disinhibition (%)	0.39 (0.38)	0 – 1	0.35 (0.36)*	0.47 (0.39)
Eating behaviours (%)	0.60 (0.30)	0 – 1	0.60 (0.28)	0.63 (0.29)
Positive/problematic behaviours	0.44 (0.27)	0 – 1	0.42 (0.27)	0.47 (0.27)
FAQ (0 – 30)	13.8 (7.2)	0 – 30	13.2 (7.1)	14.9 (7.2)
UPDRS (0 – 100) (%)	58 (11)	0 – 99	57 (10)	59 (13)

Healthy Elderly	All Subjects N = 244 Mean (SD)	Range	Males N = 133 Mean (SD)	Females N = 111 Mean (SD)
Age (Years)	69 (2)	67-77	69 (2)	69 (2)
Education (Years)	11 (2)	9-19	11 (2)	11 (2)
MMSE (0 – 30)	28.9 (1.2)	26 – 30	28.9 (1.1)	28.9 (1.2)

Significant differences between males and females: *$p < 0.05$, **$p < 0.01$.
Abbreviations: R = Right; L = Left; A = Ambidextrous; eTIV = estimated Total Intra-cranial Volume; TBV = Total Brain Volume; BF = Brain Fraction; ACE-R = Addenbrooke's Cognitive Examination Revised; MMSE = Mini-Mental State Examination; FRS = Frontotemporal Dementia Rating Scale; ADL = Activities of Daily Living; FAQ = Functional Activities Questionnaire; UPDRS = Unified Parkinson's Disease Rating Scale.

Table 2. Cortical regions with differences in the brain matter volume common to all four identified bvFTD sub-types. The group-wise differences at the whole brain level were classified by voxel-based-morphometry (VBM) against the healthy elderly group using maximum of the t-tests statistics (separated by more than 1 mm) within a cluster and then labelled according to Automated Anatomical Labelling (AAL) implemented in SPM.

Region	Sub-type (N)			
	FTP (82)	FD (41)	SL (39)	TD (51)
Limbic lobe				
Insula	●	●	●	●
Cingulate_Ant	●	●	●	●
Hippocampus	●	●	●	●
ParaHippocampal	●	●	●	●
Temporal_Pole_Sup	●	●	●	●
Sub-cortical grey nuclei				
Amygdala	●	●	●	●
Caudate	●	●	●	●
Pallidum	●	●	●	●
Thalamus	●	●	●	●
Central region				
Precentral	●	●	●	●
Frontal lobe				
Frontal_Inf_Orb	●	●	●	●
Supp_Motor_Area	●	●	●	●
Olfactory	●	●	●	●
Frontal_Sup_Medial	●	●	●	●
Rectus	●	●	●	●
Temporal lobe				
Temporal_Mid	●	●	●	●

Table 3. Cortical regions with differences in the brain matter volume specific to either of four identified bvFTD sub-types (black-filled circles). The group-wise differences at the whole brain level were classified by voxel-based-morphometry (VBM) against the healthy elderly group using maximum of the t-tests statistics (separated by more than 1mm) within a cluster and then labelled according to Automated Anatomical Labelling (AAL) implemented in SPM.

Region	Sub-type (N)			
	FTP (82)	FD (41)	SL (39)	TD (51)
Limbic lobe				
Temporal Pole Mid L	○	○	○	●
Sub-cortical grey nuclei				
Putamen	○	●	●	●
Central region				
Rolandic Oper	●	○	○	○
Postcentral	○	●	○	●
Frontal lobe				
Frontal Sup	●	●	●	○
Frontal Mid	●	●	●	○
Frontal Inf Oper	●	●	●	○
Frontal Inf Tri	●	●	●	○
Frontal Med Orb	○	●	○	○
OFCant	○	●	●	○
Temporal lobe				
Heschl L	○	○	●	○
Temporal Sup	○	○	●	○
Temporal Inf	○	○	●	○
Parietal lobe				
Parietal Sup	○	○	○	●
Parietal Inf	●	●	○	●
SupraMarginal	○	●	○	●
Angular	○	●	○	●
Precuneus	●	○	●	○
Paracental Lobule	○	○	○	○
Occipital lobe				
Occipital Sup	○	●	○	○
Occipital Mid	○	○	○	●
Occipital Inf	○	○	○	○
Fusiform	○	●	●	●

Table 4. Behavioural and cognitive variables used in the study in four bvFTD subtypes and corresponding demographic data.

Clinical Scores	Sub-type (N)				
	FTP (N=82)	FD (N=41)	SL (N=39)	TD (N=51)	*p* -value
Behavioural and Functional					
FRS	-0.45 (1.37)	**-1.10 (1.43)** [a,b]	-0.01 (1.1)	-0.10 (1.65)	0.02
Behavioural symptoms	0.42 (0.21)	**0.31 (0.19)** [c,b]	0.51 (0.19)	0.41 (0.24)	0.001
Cognition	0.36 (0.36)	0.33 (0.39)	0.33 (0.31)	0.43 (0.36)	0.54
ADL	0.52 (0.23)	**0.41 (0.23)** [a,b]	0.59 (0.22)	0.58 (0.27)	0.003
Apathy/disinterest	0.36 (0.26)	**0.25 (0.20)** [a,b]	0.47 (0.24)	**0.48 (0.27)** [d]	0.001
Eating behaviours	0.63 (0.29)	0.55 (0.27)	0.68 (0.26)	0.54 (0.27)	0.08
Disinhibition	0.42 (0.40)	**0.22 (0.30)** [c,b]	0.56 (0.34)	**0.35 (0.35)** [e]	0.004
Problem behaviours	0.47 (0.24)	**0.37 (0.25)** [b]	0.55 (0.24)	**0.35 (0.27)** [d, e]	0.001
FAQ	13.6 (7.0)	**16.6 (7.8)** [d,b]	12.0 (6.1)	12.5 (7.8)	0.02
UPDRS	59 (8)	57 (16)	58 (11)	58 (9)	0.56
Cognitive					
ACE-R	68 (17)	68 (17)	70 (18)	68 (13)	0.82
Attention	3.8 (1.5)	**3.6 (1.6)** [b]	3.8 (1.5)	4.5 (1.2)	0.02
Orientation	8.2 (2.0)	7.7 (2.2)	8.3 (2.0)	8.5 (1.7)	0.23
Category fluency	2.8 (2.1)	2.3 (2.0)	3.0 (2.1)	2.6 (1.7)	0.36
Letter fluency	2.8 (2.1)	**2.2 (1.8)** [a]	2.8 (2.1)	3.4 (1.8)	0.038
Episodic memory	13.0 (5.2)	13.4 (5.4)	12.5 (4.7)	12.6 (4.7)	0.84
Semantic memory	2.5 (1.2)	2.7 (1.2)	2.9 (1.2)	**1.8 (1.3)**[d,a,e]	<0.001
Perceptual abilities	**7.1 (1.2)** [d]	**7.0 (1.0)** [a]	7.5 (1.3)	7.8 (0.7)	0.006
Praxis	5.0 (2.4)	5.5 (2.1)	5.4 (2.6)	6.0 (2.0)	0.08
Language–phonemics	**1.3 (0.8)** [c]	1.7 (0.6)	1.6 (0.6)	1.6 (0.7)	0.013
Language–structure	6.2 (1.2)	6.0 (1.1)	6.4 (0.8)	6.1 (1.2)	0.55
Language–semantics	13.8 (3.9)	13.7 (3.6)	14.2 (2.6)	**8.9 (4.7)**[d,a,e]	<0.001
MMSE	24.5 (3.7)	23.2 (4.1)	24.5 (4.3)	25.5 (3.5)	0.09

Table 4 (continued)

Clinical Scores	FTP (N=82)	FD (N=41)	SL (N=39)	TD (N=51)	*p* -value
AChEI/Mem	64/18	34/7	29/10	44/7	0.48
Demographics					
Age	63.5 (7.5)	63.3 (7.4)	63.4 (7.3)	62.6 (7.8)	0.33
Education	14.6 (6.0)	16.0 (6.0)	15.7 (6.6)	15.0 (6.0)	0.30
Gender (M/F)	53/29	21/20	25/14	37/14	

Significant ($p < 0.05$) differences between the bvFTD subtypes in behavioural and cognitive sub-scores. FTP = frontotemporoparietal; TD = temporal-dominant; FD = frontal-dominant; SL = sub-lobar; FRS = Frontotemporal Dementia Rating Scale; ACE-R = Addenbrooke's Cognitive Examination Revised; MMSE = Mini-Mental State Examination; FAQ = Functional Activities Questionnaire; UPDRS = Unified Parkinson's Disease Rating Scale; AChEI/Mem = acetylcholinesterase inhibitor and/or memantine (1 = taking medication/s); M = Male; F = Female.

[a] differences between FD and TD

[b] differences between FD and SL

[c] differences between FD and FTP

[d] differences between TD and FTP

[e] differences between TD and SL

[f] *p*-value reported for the Pearson's Chi-square test.

Table 5. Statistical analysis: Correlation between cognitive, behaviour and functional scores and the regional core factor score. The GLM output is shown for the association between the cognitive, behavioural and functional scores and the regional factor score after adjusting for sex and subtype age and head size.

Clinical Scores	Core Factor		Core Factor			Group		
	[a] Corr.	[b] *p*	[c] F	[b] *p*	[d] Post hoc	[c] F	[b] *p*	[d] Post hoc
ACE-R	0.44	**<0.001**	22.7	**<0.001**	FTP/FD	1.43	0.24	
FAQ	-0.22	**0.001**	5.04	**0.03**	TD/FD	1.82	0.15	
MMSE	0.34	**<0.001**	9.80	**0.02**	TD/FD	0.51	0.68	
Behaviour	0.14	**0.038**	3.24	0.07		3.19	**0.03**	FD/SL
UPDRS	-0.050	0.47	0.10	0.75		0.69	0.56	

[a] Pearson correlation (Corr.) was determined for the core factor; significant values in bold.

[b] Two-tailed *p* value.

[c] A GLM used to analyse the output by core factor and by group; significant values in bold.

[d] Post-hoc analysis for group differences significant at $p < 0.05$

Abbreviations: ACE-R = Addenbrooke's Cognitive Examination Revised; FAQ = Functional Activities Questionnaire; FTP = frontotemporoparietal; FD = frontal-dominant; GLM = General Linear Model; MMSE = Mini-Mental State Examination; Behaviour = Behavioural sub-score from Frontotemporal Dementia Rating Scale; SL = sub-lobar; TD = temporal-dominant; UPDRS = Unified Parkinson's Disease Rating Scale.

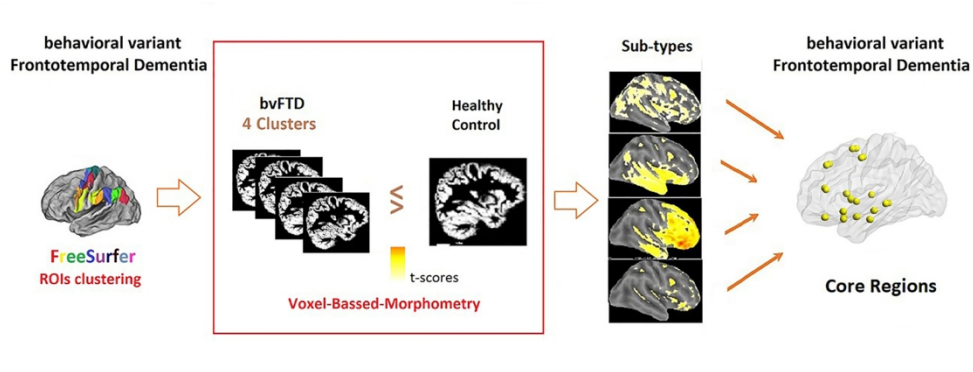

152x56mm (300 x 300 DPI)

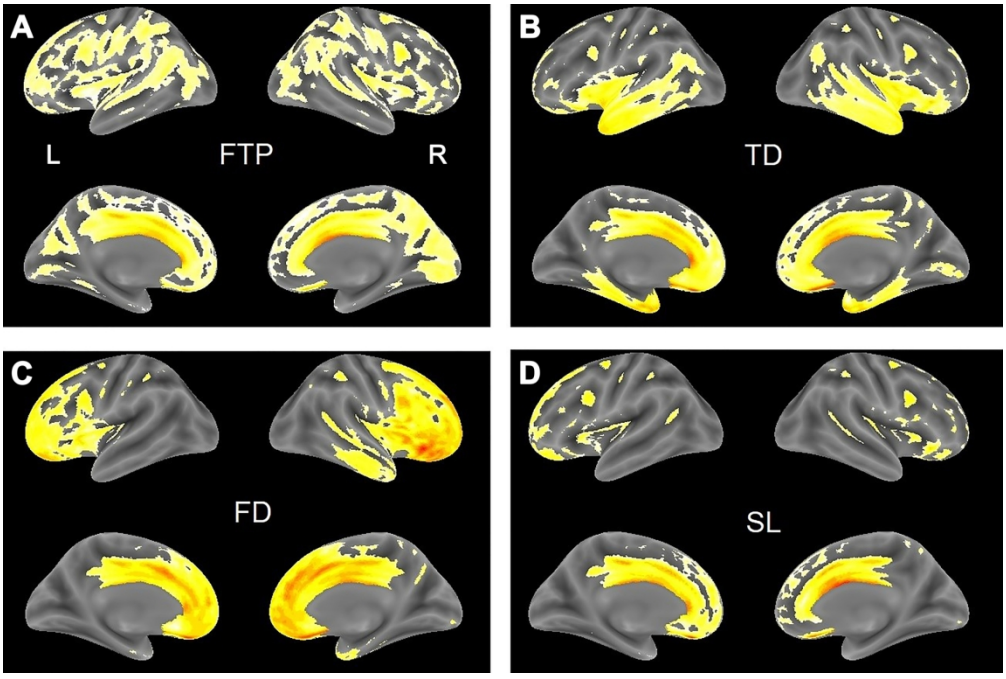

162x108mm (300 x 300 DPI)

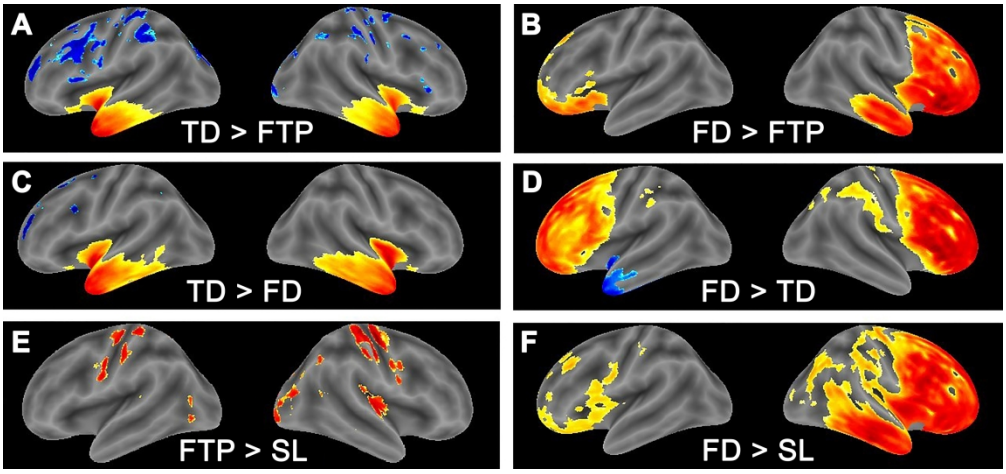

338x157mm (300 x 300 DPI)

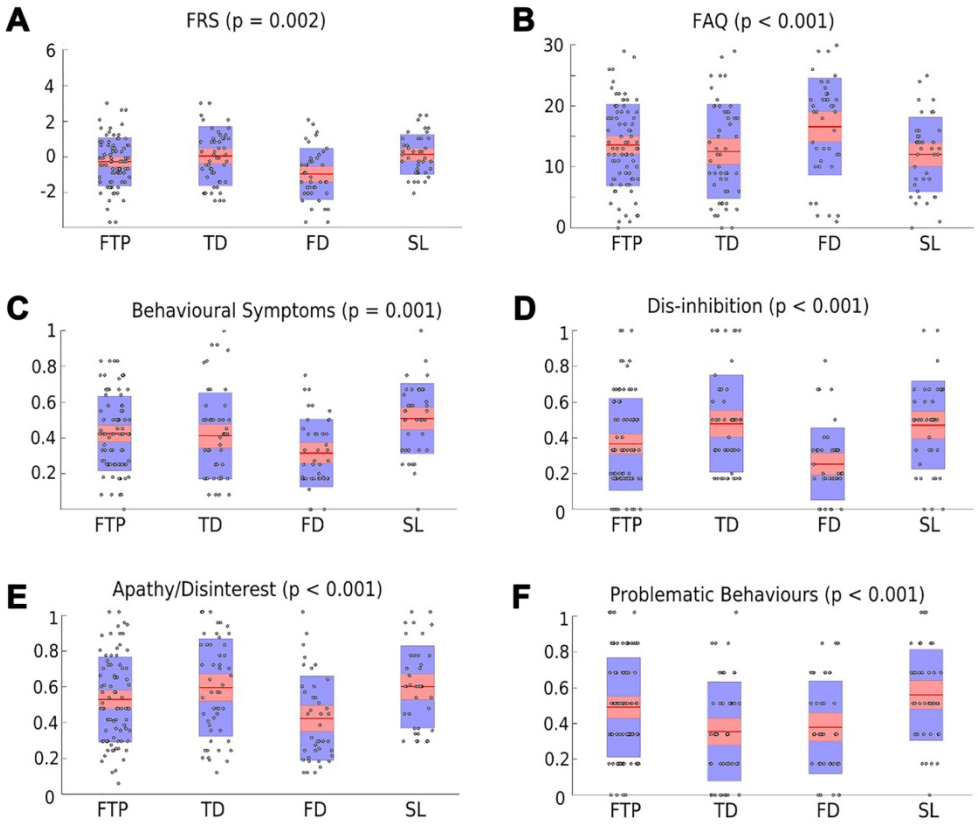

152x131mm (300 x 300 DPI)

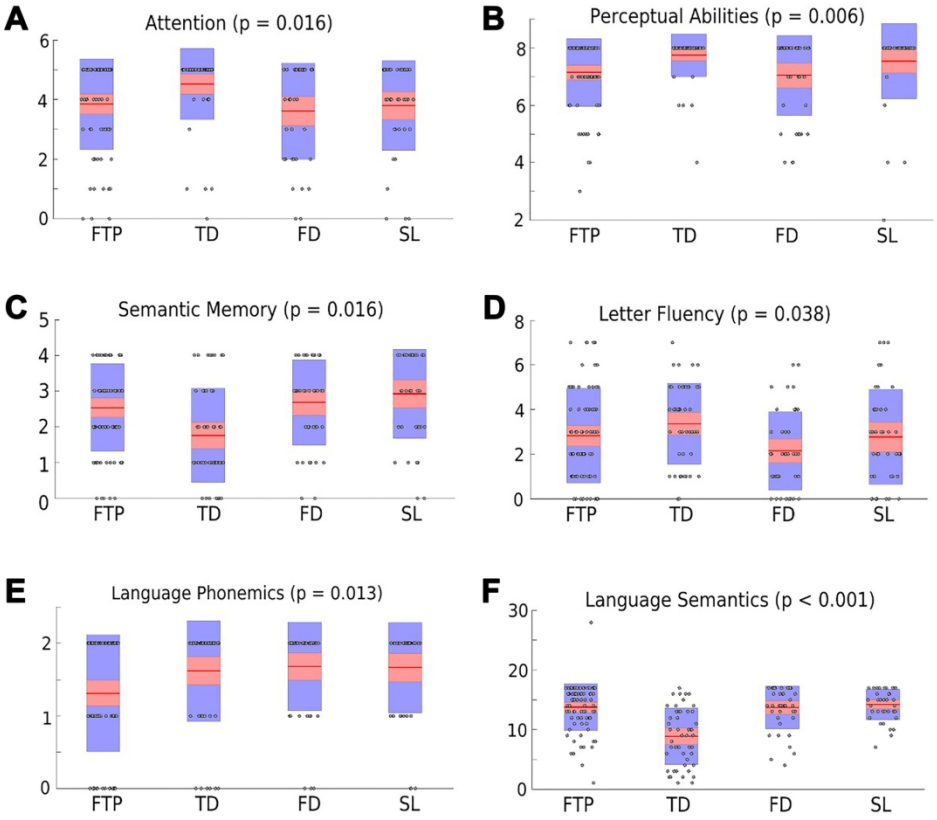

162x140mm (300 x 300 DPI)

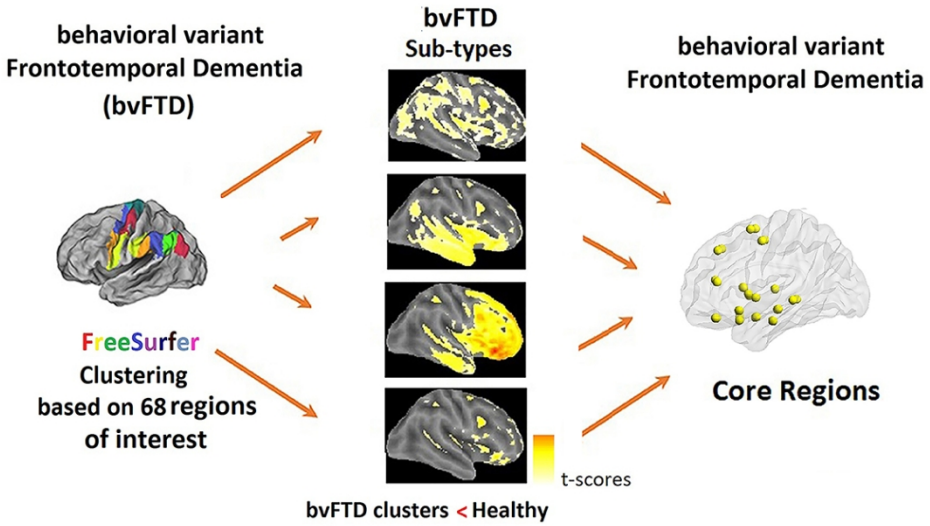

Graphical Abstract

Degeneration of basal and limbic networks is a core feature of behavioural variant frontotemporal dementia

Vesna Vuksanović, Roger T. Staff, Suzannah Morson, Trevor Ahearn, Luc Bracoud, Alison D. Murray, Peter Bentham, Christopher M. Kipps, Charles R. Harrington and Claude M. Wischik

Abbreviated summary

Using trial baseline MRI scans from 213 behavioural variant frontotemoporal dementia patients, Vuksanovic *et al.* report that the four known cortical atrophy subtypes all share degeneration in core basal, limbic and frontal network hubs that correlates with cognitive and functional impairment irrespective of subtype.